THE JOURNAL OF PHYSICAL CHEMISTRY A LETTERS

2008, *112,* 13282–13286
Published on Web 11/21/2008

EDOT-Type Materials: Planar but Not Rigid

Begoña Milián Medina,[†] Dorothee Wasserberg,[‡] Stefan C. J. Meskers,[‡] Elena Mena-Osteritz,[§] Peter Bäuerle,[§] and Johannes Gierschner*[,∥,⊥]

Institut de Ciència Molecular (ICMOL), University of Valencia, P.O. Box 22085, 46071 Valencia, Spain, Molecular Materials and Nanosystems, Eindhoven University of Technology, P.O. Box 513, 5600 MB Eindhoven, The Netherlands, Institute of Organic Chemistry II and Advanced Materials, University of Ulm, Albert-Einstein-Allee 11, 89081 Ulm, Germany, Madrid Institute for Advanced Studies, IMDEA Nanoscience, UAM, Modulo C-IX, Av. Tomás y Valiente 7, Campus de Cantoblanco, 28049 Madrid, Spain, and Institute for Physical and Theoretical Chemistry, University of Tübingen, Auf der Morgenstelle 8, 72076 Tübingen, Germany

Received: October 31, 2008

The geometrical, electronic and optical properties of α,α′-quater(3,4-ethylenedioxythiophene) (4EDOT) and α,α′-quater(thiophene) (4T) are studied by quantum-chemical calculations; the computed vibronic spectra at low and room temperature (RT) are compared to experiment. Our results suggest that the better resolved RT absorption spectrum of 4EDOT in comparison with 4T is not due to the molecule's rigid nature as commonly assumed but due to very similar out-of-plane modes in the electronic ground and first excited states of 4EDOT, with low frequencies indicative of its rather soft nature.

Introduction

3,4-Ethylenedioxythiophene (EDOT) has been used as a building block for the synthesis of functional conducting polymers with interesting electrochemical and electro-optical properties.[1] Its specific strong electron donor properties make it interesting as a building block for the design of low band gap π-conjugated systems with applications in electro-optical devices such as organic light-emitting diodes and solar cells.[2] An interesting aspect of EDOT-type materials is its proposed "self-rigidification".[3,4] This is suggested to arise from attractive sulfur−oxygen interactions and to be the reason for the well-structured absorption spectra,[4−7] compared to unsubstituted oligothiophenes (*n*Ts), which at room temperature show only vibronic structure in emission, but broad featureless absorption spectra.[8,9]

It was shown in earlier combined experimental and quantum-chemical work that the broad absorption of unsubstituted *n*Ts arises from thermal population of torsional modes, where these modes exhibit a much more shallow potential in the electronic ground state (S_0) compared to the first excited-state S_1.[9,10] The important feature—the large increase in the force constant (and thus frequency) of the torsional modes upon electronic excitation—arises from the enhanced double bond character of the bonds linking the thiophene rings in the S_1 state. Upon lowering the temperature,[9−11] or placing the molecule in a rigid environment,[12,13] thermal population of torsional modes becomes negligible and the broad featureless absorption transforms into a well-resolved spectrum showing vibrational progressions, and mirror-symmetric absorption and fluorescence spectra are obtained.[9]

Following this idea, we will thus investigate in this contribution the geometrical, electronic, and optical properties of the four-unit oligomer 4EDOT (and for consistency of 4T) in a full quantum-chemical approach to elucidate the reason for the well-structured absorption spectrum and give an answer to the question of self-rigidification in EDOT-type materials.

Materials and Methods

The experimental absorption and emission spectra of 4T and trimethylsilyl end-capped 4EDOT (4EDOT-TMS_2) at low and room temperature (RT) in solution are depicted in Figure 1. The spectra of 4EDOT-TMS_2 were recorded in MeTHF at 80 K and RT. The spectra of 4T were recorded in tetradecane at 12 K and RT. The terminal TMS groups are needed to chemically stabilize 4EDOT.[6] In the calculations, the TMS groups were replaced by hydrogen atoms to reduce the computational time, because the substituents are not expected to substantially affect neither the vibronic structure nor the spectral position by a large extent.[6] The equilibrium geometries, the highest occupied and lowest unoccupied molecular orbitals (HOMO, LUMO), the vibrational frequencies of the S_0 and S_1 states, the adiabatic and vertical transition energies, and the emission and absorption spectra were calculated at the (time-dependent) density functional (TD)DFT level, using the hybrid BHLYP functional and the standard 6-31G* basis set. The geometries of the thiophene backbones were set planar (C_{2h} and C_2 symmetry for 4T and 4EDOT, respectively). No frequency scaling was applied to derive the theoretical spectra. All calculations were performed in vacuo, using the TURBOMOLE program.[15] The Huang−Rhys (HR) factors and Duschinsky

* Corresponding author. E-mail: johannes.gierschner@imdea.org.
[†] University of Valencia.
[‡] Eindhoven University of Technology.
[§] University of Ulm.
[∥] IMDEA Nanoscience.
[⊥] University of Tübingen.

10.1021/jp809632z CCC: $40.75

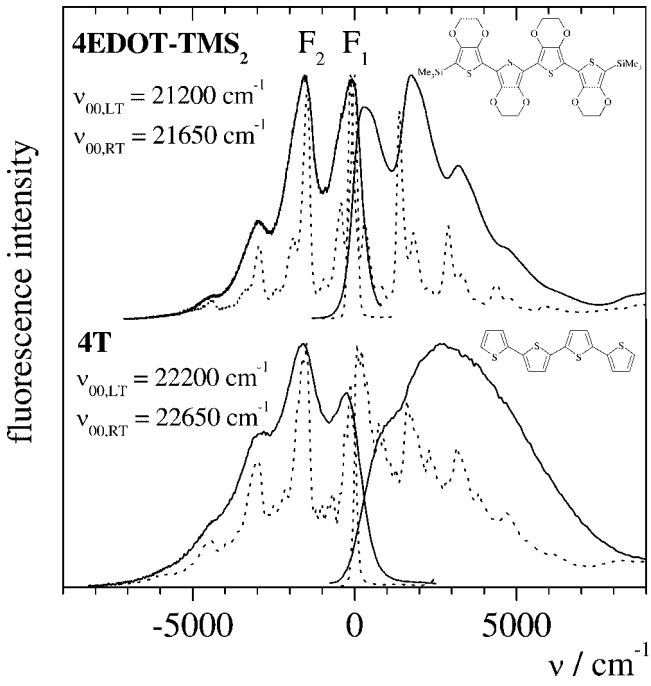

Figure 1. Experimental fluorescence (left) and absorption (right) spectra of 4EDOT-TMS_2 and 4T at low (dotted lines) and room (solid lines) temperature.[14] For better comparison, the abscissa scale is normalized to the electronic origin ν_{00}. The blue-shift of ν_{00} upon increasing the temperature is due to the change in the polarizability (see ref 9).

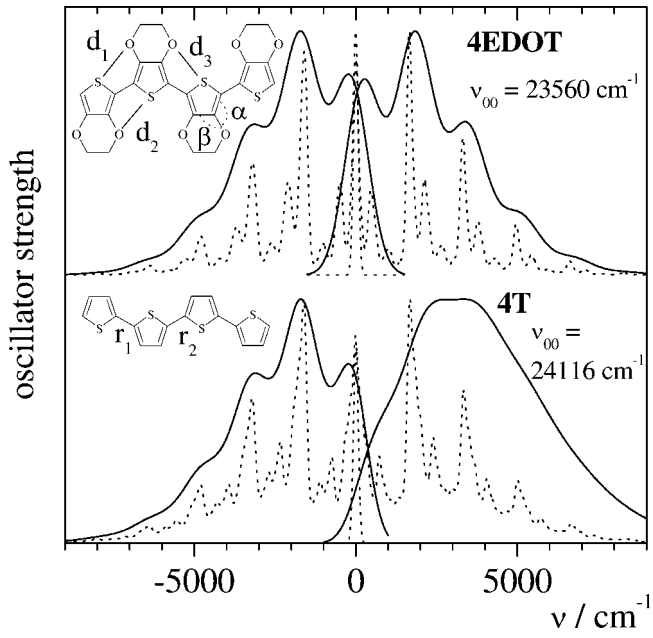

Figure 2. Calculated fluorescence (left) and absorption spectra (right) of 4EDOT and 4T from BHLYP/6-31G* calculations according to eqs 1 and 2 and ref 10. Dashed lines: low temperature simulation with inserted Gaussian half-width $\gamma = 150$ cm^{-1}. Solid lines: room temperature convolution at 293 K with $\gamma = 800$ cm^{-1} and $\nu_0 = 11$, 21, 25, 40, 54 cm^{-1} and $\nu_1 = 10$, 29, 33, 50, 55 cm^{-1} (4EDOT) and $\nu_0 = 16$, 30, 48 cm^{-1} and $\nu_1 = 103$, 110, 125 cm^{-1} (4T). An additional broadening with $\gamma = 800$ cm^{-1} (4EDOT) and $\gamma = 500$ cm^{-1} (4T) has been performed to better reproduce the experiment. For better comparison, the abscissa scale is normalized to the electronic origin ν_{00}.

matrix elements (DME) were calculated with the DUSHIN program.[16] All calculations for the simulation of the optical spectra were done using in-house programs.

Results and Discussion

a. Low Temperature Spectra. The first step to calculate the optical spectra on a quantum-chemical basis is to compute the coupling between the electronic transition and the vibrational normal modes, determined by the Franck−Condon (FC) factors. At low temperature (LT), the vibronic coupling will be most effective with totally symmetrical in-plane modes because in these modes the displacements are large. If the geometry change upon electronic excitation is small, such normal modes are well described within the displaced undistorted harmonic oscillator model (linear coupling)[17] and thus, the spectra can be obtained by a procedure described, e.g., in ref 10. The FC factors within this approximation for transitions from vibrational quanta m in the initial state to quanta n in the final state, for a totally symmetrical mode k, at $T = 0$ K ($m = 0$) are given by

$$F^2_{n0}(k) = \frac{(S_k)^{n_k} e^{-S_k}}{n_k!} \qquad (1)$$

S_k are the Huang−Rhys factors, which are obtained from the projection of the geometrical change upon electronic excitation on the normal coordinates associated with the vibrational modes.[18] The stick spectrum is obtained by calculating all intercombinations of the modes. The spectra are then simulated with a Gaussian function of width at half-height γ to account for the dynamic inhomogeneity of the environment. Note that γ is the only adjustable parameter in this approach. The simulated low temperature spectra (see Figure 2) reproduce well the experimental ones (Figure 1), which is consistent with earlier studies.[9,10,19,20] At low temperature, 4T exhibits well-structured fluorescence and absorption spectra, which reveal that only a few vibrational modes couple effectively to the electronic transition.[8,21] As previously observed,[21] the vibronic progressions in 4T are mainly based on two stretching modes labeled a and b, with frequencies $\nu_a = 166$ cm^{-1} and $\nu_b = 1585$ cm^{-1}, as calculated for the S_0 state; see Table 1.

TABLE 1: Selected Modes for 4T: Calculated Vibrational Frequencies (in cm^{-1}), for a Given Normal Mode k in the Excited State, of the Ground (ν_0) and First Excited State (ν_1), Symmetry, Duschinsky Matrix Element (DME), Description, Distortion R, and Huang−Rhys Factors S_k for Absorption (Force Constant for the Torsional Normal Modes in Parentheses (in 10^{-3} mDyne/Å))

k	ν_1	ν_0	symmetry	description	DME (%)	$\lvert R\rvert$ (%)	S_k
				In-Plane			
2	59	45	b_u	in-plane bending	100	13	0
6	119	109	a_g	in-plane bending	99	4	0.01
8	167	166	a_g	in-plane stretching	97	0	0.64
10	180	177	b_u	in-plane bending	94	0	0
14	344	334	a_g	in-plane bending	86	1	0.25
30	721	735	a_g	intra-ring stretching	30	1	0.33
74	1666	1585	a_g	inter/intra-ring stretching	27	2	1.03
				Out-of-Plane			
3	87	76	b_g	butterfly	90	7	0
4	103 (43.0)	16[a] (0.8)	a_u	torsion	73	73	0
5	110 (48.7)	30[a] (3.1)	b_g	torsion	73	57	0
7	125 (62.7)	48[a] (10.3)	a_u	torsion	80	45	0

[a] Reference 25.

At a first glance, the vibronic pattern in 4EDOT looks similar, dominated by a strong peak around 1600 cm^{-1},[6] which is actually due to two different modes ($k = 135$, 136) with very similar nuclear displacements and frequencies, see Table 2. The mode at $\nu = 154$ cm^{-1}, is similar to the a mode in 4T, but

TABLE 2: Selected Modes for 4EDOT: Calculated Vibrational Frequencies (in cm^{-1}), for a Given Normal Mode k in the Excited State, of the Ground (ν_0) and First Excited State (ν_1), Symmetry, Duschinsky Matrix Element (DME), Description, Distortion R, and Huang−Rhys Factors S_k for Absorption (Force Constant for the Out-of-Plane Normal Modes in Parentheses (in 10^{-3} mDyna/Å))

k	ν_1	ν_0	symmetry	description	DME (%)	|R| (%)	S_k
				In-Plane			
4	34	35	b	in-plane bending	97	1	0
7	64	65	a	in-plane bending	87	1	0
17	154	162	a	in-plane stretching/bending	47	3	0.03
18	163	154	a	in-plane stretching	47	3	0.18
40	464	441	a	intra-ring stretching (+inter-ring bending)	11	3	0.32
54	603	441	a	intra-ring stretching	18	16	0.10
135	1651	1554	a	in-plane stretching	27	3	0.78
136	1660	1609	a	in-plane stretching	15	2	0.20
				Out-of-Plane			
1	10 (0.3)	11 (0.4)	a	torsion+butterfly	99	5	0
2	29 (3.9)	21 (2.2)	a	torsion+butterfly	90	16	0
3	33 (3.8)	25 (2.2)	b	torsion	95	14	0
5	50 (8.1)	40 (5.7)	a	torsion+butterfly	89	11	0
6	55 (14.1)	54 (12.7)	b	butterfly	92	1	0
8	76 (23.3)	78 (24.4)	a	butterfly	91	1	0

couples less strongly to the electronic transition. In 4EDOT, this mode necessarily contains nuclear displacements within the ethylenedioxy units whereas in 4T it is located within the thiophene backbone. Because the geometrical change upon electronic excitation is exclusively localized in the thiophene backbone, the coupling of this mode in 4T is significantly stronger. This accounts in general for the vibronic pattern in 4EDOT, thus revealing a smaller reorganization energy, which can be seen from the significant decrease of the ratio of the high energy sub-bands F_2/F_1 in the emission spectra of 4EDOT compared to 4T; see Figure 1. Quantitative determination of the reorganization energy[10] from the experimental emission spectrum $I(\nu)$, which corresponds to the difference between the vertical (ν_{vert}) and adiabatic transition energy (electronic origin; ν_{00}),

$$\Delta\nu = \nu_{00} - \nu_{vert} = \nu_{00} - \frac{\int I(\nu)\nu \, d\nu}{\int I(\nu) \, d\nu} \qquad (2)$$

yields $\Delta\nu_{exp} = 1700\ cm^{-1}$ for 4EDOT, but $\Delta\nu_{exp} = 2100\ cm^{-1}$ for 4T. The DFT calculations yield higher values ($\Delta\nu_{4EDOT} = 2100\ cm^{-1}$, $\Delta\nu_{4T} = 2400\ cm^{-1}$); however, they show the same qualitative trend.

b. Room Temperature Spectra. Starting from the LT spectra, simulation of RT spectra has to take into account the increase in inhomogeneous broadening due to interactions with the environment via a larger Gaussian half-width γ.[10] In a second step, thermal population of higher vibrational levels of the initial electronic state i has to be included; this changes the overall intensity distribution of excitations to the various vibrational levels of the final electronic state f. At room temperature, only modes with $h\nu \lesssim k_B T$ (where h is the Planck constant, k_B is the Boltzmann constant and T is the temperature) are thermally accessed and thus only modes with $\nu \lesssim 200\ cm^{-1}$ are considered in the calculation.

When calculating the effect of thermal population, we distinguish between totally symmetric modes and out-of-plane modes. Totally symmetric modes are found to contribute little to the broadening in comparison to the effect of the environment (γ) and can be neglected. In contrast, non totally symmetric out-of-plane modes, which are not displaced when going from the initial to the final state in the approximation used here, contribute significantly to the thermal broadening. These modes can couple with the electronic excitation when the frequency differs in the initial and final state (distortion). In this quadratic coupling case,[17] transitions between states i and f of thermally populated vibrational quanta can be calculated either in a semiclassical approach, where the different curvature of the modes in i and f give rise to an exponential distribution function,[10,17,22] or by a full quantum-chemical approach. Here, the FC factors F_{nm}^2 of transitions between quantum numbers m, n of the torsional frequencies (ν_i, ν_f) in the initial and final electronic states, respectively, are calculated by a recursion formula[23] based on the expression for excitations at 0 K[18] (i.e., $m = 0$)

$$F_{n0}^2 = (1-R^2)^{1/2} R^n \frac{(1)(3)(5)...(n-1)}{(2)(4)(6)...(n)}, \text{ for } n \text{ even}$$
$$F_{n0}^2 = 0, \text{ for } n \text{ odd} \qquad (3)$$

where $R = (\nu_i - \nu_f)/(\nu_i + \nu_f)$ is the relative distortion of the frequencies ν from state i to f for a given normal mode k against their mean. The intensity distribution for a given temperature is then calculated by populating the initial vibrational states m according to Boltzmann. The impact on the spectrum will be large if R is large. Appropriate candidates are typically torsional modes. Other out-of-plane modes, on the other hand, like butterfly modes, show only small distortions (see Table 1) and usually do not have to be considered.

In the case of 4T, the low-frequency out-of-plane normal modes in both the ground and excited states can be essentially described by local motions, e.g., "torsions" and "butterfly"; see Table 1. Mode-mixing[24] is typically small and consequently the Duschinsky matrix elements connecting the modes in the ground and excited states are close to unity (Table 1). For all the normal modes except for torsions, R is very small and the coupling is sufficiently described by eq 1. For torsional modes,[25] the HR factors are zero and the distortions are large with $R = 45-73\%$ (Table 1); thus eq 3 is valid. The simulated 4T spectra, shown in Figure 2, reproduce well the changes observed experimentally (Figure 1): Increasing the temperature results in a broadening with loss of mirror symmetry and the appearance of a broad structureless absorption band, accompanied by a considerable blue-shift, as previously observed for systems with large degrees of torsional freedom.[8,9,26] This effect arises from the different rigidity of the molecular backbone in the ground and excited states, here due to a substantial shortening of the inter-ring bond length upon electronic excitation; see Table 3. Therefore, the force constants, and thus the frequencies associated with torsional motion, become larger in S_1 compared to S_0 (Table 1). Hence, thermal population in S_0 causes a wider spectral distribution function compared to S_1 and therefore a stronger blurring and blue-shift for absorption as compared to fluorescence.

TABLE 3: Inter-ring Bond-Lengths r_i of 4T and 4EDOT and S···O Distances d_i of 4EDOT (in Å) in S_0 and S_1 Calculated at the BHLYP/6-31G* level (r_i and d_i Given in Figure 2)

		inter-ring bonds		S···O distances		
		r_1	r_2	d_1	d_2	d_3
4T	S_0	1.447	1.444			
	S_1	1.413	1.388			
4EDOT	S_0	1.440	1.438	2.927	2.939	2.934
	S_1	1.408	1.387	2.908	2.930	2.912

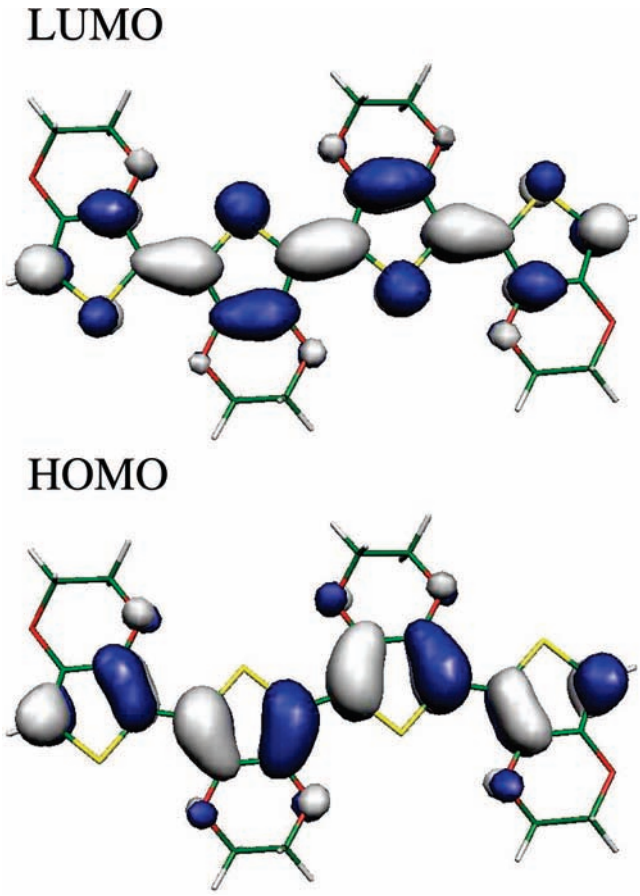

Figure 3. Electronic density contours (0.04 e/bohr^3) calculated for the HOMO and the LUMO of 4EDOT (ref 27).

The same procedure is applied to 4EDOT. However, it is difficult to assign the torsional modes: the normal modes in S_0 and S_1 need to be described as a combination of local motions (see Table 2). In any case, the nuclear displacements of a given out-of-plane mode are very similar in S_0 and S_1, as can be seen from the high DME values, which are close to unity. To simulate the room temperature spectra, we have thus applied eq 3 to the first six out-of-plane modes (see Table 2). Again, the simulated spectra reproduce well the changes observed with increasing temperature, namely, broadening of the spectra, whereas, in this case, the vibrational fine structure is still observed in both the emission and absorption spectra (see Figures 1 and 2). The reason is readily seen from Table 2: the distortion of the out-of-plane modes is small, yielding small *R*, a direct result of the fairly similar force constants (and thus frequencies) in S_0 and S_1, for all low-frequency out-of-plane modes.

Similar force constants are induced by the combination of two opposite effects: on the one hand, a geometrical effect due to the shortening of the inter-ring bonds upon electronic excitation, which is essentially the same as in 4T (see Table 3) (the increase of the rigidity in S_1 will increase the force constants for the ring torsions in S_1 with respect to S_0, as previously described for 4T); on the other hand, an electronic effect, which can be seen in the topologies of the HOMO and LUMO orbitals (see Figure 3), because the first electronic transition is well described by a HOMO $\rightarrow$ LUMO excitation. In the HOMO, no bonding interaction between sulfur and oxygen is found because the LCAO coefficients of sulfur are essentially zero (alike in 4T), whereas in the LUMO an antibonding (repulsive) interaction is observed, which lowers the force constant in S_1. The compensation of these two opposite effects leads to substantially similar force constants of the torsional potentials in both electronic states.

Most importantly, the force constants for the torsions in 4EDOT are very similar to the *ground state* of 4T, and not to its excited state (see Tables 1 and 2), as one might expect from the self-rigidification paradigm.[3,4] The latter was drawn from the short S···O distances, which amount to 2.96 Å on average as found in the crystal structures;[3b,4] our calculations give ca. 2.94 Å for S_0; see Table 3. This is shorter than the van der Waals distance between S and O (3.35 Å), and it was thus assumed to be driven by attractive S···O interactions.[28] However, comparison of the one-unit monomer 1EDOT with oligomer 4EDOT at the DFT level reveals very similar geometries in the thiophene and the ethylenedioxy moiety. Furthermore, the inter-ring bonds in 4EDOT, for which $r =$ 1.44 Å is yielded, are only slightly shorter (less than 0.01 Å) than those in 4T; see Table 3. Therefore, the S···O distances are largely dictated by the intra-ring constraints within the EDOT unit and by the inter-ring bond length.

Further evidence for nonbonding S···O interaction in the electronic ground state of EDOT-type materials arises from an analysis according to Raos et al.,[29] following the change $\Delta = (\beta - \alpha)_{180°} - (\beta - \alpha)_{90°}$ of the bond angles α, β between oxygen and the thiophene ring (Figure 2) along the torsional coordinate where 180°, 90° correspond to trans-planar and perpendicular conformations, respectively. The small negative value of $\Delta = -0.03$[30] points to an essentially nonbonding S···O interaction, where opposite charges on S (δ^+) and O (δ^-) compensate sterical repulsion.[31] For the unsubstituted species, significant repulsive interaction is observed,[29] yielding $\Delta = -1.37$, which might mainly arise from the rejection of positive partial charges on S and H rather than sterical hindrance.[32] This difference in the S···O and S···H interactions in nEDOT and nT, respectively, are held responsible for the different gas-phase equilibrium geometries in the electronic ground state: while 4EDOT is calculated to be coplanar, geometry optimization of 4T yields a distorted structure with inter-ring dihedral angles of typically 10−30° at the DFT level (depending somewhat on functional and basis set).[26] Hence, from the geometry and from the torsional force constants in the ground-state compared to 4T, 4EDOT has to be reconsidered as a planar, but *soft*, *nonrigidified molecule*. Its well-resolved absorption spectrum arises not from rigidification, but from an "electronic softening" upon electronic excitation, which compensates the usual geometrical "hardening" in oligothiophenes upon electronic excitation.

Conclusions

We have provided a quantum-chemical approach to understand the well-structured room-temperature absorption spectrum of the 4EDOT oligomer by a thorough comparison with the unsubstituted species (4T), which exhibits an unstructured spectrum. We have stressed that the shape of the spectrum arises from the *change* of the geometrical and vibrational properties upon electronic excitation and cannot be predicted from the properties of the ground state alone, but requiring the complete knowledge of electronic structure, geometries, and thermally populated vibrations of the electronic states involved. We have demonstrated that the well resolved spectral features of 4EDOT are due to very similar out-of-plane modes in the electronic ground (S_0) and first excited state (S_1), which exhibit surprisingly low frequencies. Our calculations thus reveal that EDOT-type materials are not rigid systems, but have to be considered as "soft" materials rather similar to the unsubstituted species.

Acknowledgment. This work was supported by the European Commission through the Human Potential Programme (Marie-Curie RTN NANOMATCH, Grant No. MRTN-CT-2006-035884) and by the Ministerio de Educación y Ciencia of Spain (MEC) through the Project CTQ2006-14987-C02-02. B.M.M. thanks the MEC for a "Juan de la Cierva" contract. J.G. is a "Ramón y Cajal" Research Fellow, financed by the MEC. We are grateful to Prof. J. R. Reimers (University of Sidney, Australia) for making available a version of his recently developed DUSHIN program, and K. Zojer (Technische Universität Graz, Austria) for adapting TURBOMOLE output files to the DUSHIN input.

References and Notes

(1) (a) Groenendaal, L. B.; Zotti, G.; Aubert, P. -H.; Waybright, S. M.; Reynolds, J. L. *Adv. Mater.* **2003**, *15*, 855. (b) Groenendaal, L. B.; Jonas, F.; Freitag, D.; Pielartzik, H.; Reynolds, J. L. *Adv. Mater.* **2000**, *12*, 481.

(2) (a) Roncali, J. *Macromol. Rapid Commun.* **2007**, *28*, 1761. (b) Roncali, J.; Blanchard, P.; Frère, P. *J. Mater. Chem.* **2005**, *15*, 1589.

(3) (a) Turbiez, M.; Frère, P.; Blanchard, P.; Roncali, J. *Tetrahedron Lett.* **2000**, *41*, 5521. (b) Turbiez, M.; Frère, P.; Allain, M.; Videlot, C.; Ackermann, J.; Roncali, J. *Chem. Eur. J.* **2005**, *11*, 3742.

(4) Turbiez, M.; Frère, P.; Roncali, J. *J. Org. Chem.* **2003**, *68*, 5357.

(5) Apperloo, J. J.; Groenendaal, L.; Verheyen, H.; Jayakannan, M.; Janssen, R. A.; Dkhissi, A.; Beljonne, D.; Lazzaroni, R.; Brédas, J.-L. *Chem. Eur. J.* **2002**, *8*, 2384.

(6) Wasserberg, D.; Meskers, S. C. J.; Janssen, R. A.; Mena-Osteritz, E.; Bäuerle, P. *J. Am. Chem. Soc.* **2006**, *128*, 17007.

(7) Perepichka, I. P.; Roquet, S.; Leriche, P.; Raimundo, J.-M.; Frère, P.; Roncali, J. *Chem. Eur. J.* **2006**, *12*, 2960.

(8) (a) Fichou, D., Ed. *Handbook of Oligo- and Polythiophenes*; Wiley-VCH: Weinheim, 1999; (b) Becker, R. S.; Seixas de Melo, J.; Maçanita, A. L.; Elisei, F. *J. Phys. Chem.* **1996**, *100*, 18683. (c) DiCesare, N.; Belletête, M.; Leclerc, M.; Durocher, G. *Chem. Phys. Lett.* **1998**, *291*, 487.

(9) Gierschner, J.; Mack, H.-G.; Egelhaaf, H.-J.; Schweizer, S.; Doser, B.; Oelkrug, D. *Synth. Met.* **2003**, *138*, 311.

(10) Gierschner, J.; Mack, H.-G.; Lüer, L.; Oelkrug, D. *J. Chem. Phys.* **2002**, *116*, 8596.

(11) Birnbaum, D; Kohler, B. E. *J. Chem. Phys.* **1989**, *90*, 3506.

(12) Gierschner, J.; Lüer, L.; Oelkrug, D.; Musluoglu, E.; Behnisch, B.; Hanack, M. *Adv. Mater.* **2000**, *12*, 757.

(13) Bongiovanni, G.; Botta, C.; Di Silvestro, G.; Loi, M. A.; Mura, A.; Tubino, R. *Chem. Phys. Lett.* **2001**, *345*, 386.

(14) The absorption and emission spectra of 4EDOT-TMS_2 have been recorded in frozen MeTHF at 80 K and in dichloromethane at room T, and have been taken from ref 6. The absorption and emission spectra of 4T have been recorded in tetradecane at 12 and 290 K.

(15) TURBOMOLE 5.7.1 quantum-chemical package: Electronic Structure Calculations on Workstation Computers: The Program System TURBOMOLE. Ahlrichs, R.; Bär, M.; Häser, M.; Horn, H.; Kölmel, C. *Chem. Phys. Lett.* **1989**, *162*, 165.

(16) Reimers, J. R.; Cai, Z.-L.; Bilic, A.; Hush, N. S. *Ann. N. Y. Acad. Sci.* **2003**, *1006*, 235.

(17) Sluch, M. I.; Godt, A.; Bunz, U. H.; Berg, M. A. *J. Am. Chem. Soc.* **2001**, *123*, 6447.

(18) (a) Manneback, C. *Physica* **1951**, *17*, 1001. (b) Siebrand, W. *J. Chem. Phys.* **1967**, *46*, 440.

(19) Karabunarliev, S.; Baumgarten, M.; Bittner, E. R.; Müllen, K. *J. Chem. Phys.* **2000**, *113*, 11372.

(20) Dierksen, M.; Grimme, S. *J. Chem. Phys.* **2004**, *120*, 3544.

(21) Birnbaum, D.; Fichou, D.; Kohler, B. E. *J. Chem. Phys.* **1992**, *96*, 165.

(22) Myers, A. B.; Trulson, M. O.; Mathies, R. A. *J. Chem. Phys.* **1985**, *83*, 5000.

(23) The general recursion formula for displaced distorted harmonic oscillators reads

$$F^2_{n,m} = \left(-\sqrt{(m-1)R^2F^2_{n,m-2}} + \sqrt{n(1-R^2)F^2_{n-1,m-1}} - \sqrt{S(1+R)F^2_{n,m-1}}\right)^2/m$$

as given in: Henry, B. R.; Siebrand, W. In *Organic Molecular Photophysics*; Birks, J. B., Ed.; John Wiley & Sons Ltd.: Bristol, U.K., 1973; p 218.

(24) Duschinsky, F. *Acta Physicochem. URSS* **1937**, *7*, 551.

(25) In the case of 4T, the torsional frequencies of the ground state were taken from a non-planar C_2 equilibrium geometry because the torsional frequencies of the planar structure were found to be non-real as a result of performing the calculations in vacuo. The suitability of the frequencies of the C_2 conformer arises from the almost identical geometries of both structures, and the small dihedral angles between the thiophene rings in the C_2 conformer (15−20°).

(26) Macchi, G.; Milián Medina, B.; Zambianchi, M.; Tubino, R.; Cornil, J.; Barbarella, G.; Gierschner, J.; Meinardi, F. *Phys. Chem. Chem. Phys.* **2008**, DOI:10.1039/B810915J.

(27) The MOs have been depicted using the MOLEKEL 4.3 program: Flükiger, P.; Lüthi, H. P.; Portmann, S.; Weber, J. Swiss Center for Scientific Computing, Manno, Switzerland, 2000−2002. Portmann, Stefan; Lüthi, Hans Peter. MOLEKEL: An Interactive Molecular Graphics Tool. *CHIMIA* **2000**, *54*, 766.

(28) S···O distances from X-ray data of EDOT type materials range from 2.91 to 3.03 Å,[3b,4] with an average of 2.96 Å. The somewhat longer S···O distances (ca. 3.06 Å) in mixed thiophene-EDOT compounds (ref 3b) arise mainly from the fact that the structures are not planar but show torsional dihedral angles of about 14°.

(29) Raos, G.; Famulari, A.; Meille, S. V.; Gallazzi, M. C.; Allegra, G. *J. Phys. Chem. A* **2004**, *108*, 691.

(30) For 2EDOT model calculation at the BHLYP/cc-pVTZ level gives $\alpha = 124.02°$, $\beta = 121.93°$ for TP and $\alpha = 124.00°$, $\beta = 121.94°$ for 90°, $\Delta = -0.03$. For 2T, $\alpha = 123.15°$, $\beta = 123.36°$ for TP and $\alpha = 122.53$, $\beta = 124.11°$ for 90°, $\Delta = -1.37$ is obtained.

(31) This attractive force can vary significantly; e.g., Raos et al.[29] calculated $\Delta = +0.60$ for dimethoxy-substituted 2T.

(32) Note that the S···H distance in planar 2T optimized at the BHHLYP/cc-pVTZ level of theory under symmetry constraints (C_{2h}) yields 2.92 Å, not much smaller than the van der Waals distance (3.05 Å).

JP809632Z